Immunity
Article

The Ubiquitin Modifying Enzyme A20 Restricts B Cell Survival and Prevents Autoimmunity

Rita M. Tavares,[1,2,5] Emre E. Turer,[1,5] Chih L. Liu,[3] Rommel Advincula,[1] Patrizia Scapini,[4] Lesley Rhee,[1] Julio Barrera,[1] Clifford A. Lowell,[4] Paul J. Utz,[3] Barbara A. Malynn,[1,6,*] and Averil Ma[1,6,*]
[1]Department of Medicine, University of California, San Francisco, San Francisco, CA
[2]PhD Program in Biomedicine, Instituto Gulbenkian de Ciência, Oeiras, Portugal
[3]Department of Medicine, Stanford University School of Medicine, Stanford, CA
[4]Department of Laboratory Medicine, University of California, San Francisco, San Francisco, CA
[5]These authors contributed equally to this work
[6]These authors contributed equally to this work
*Correspondence: averil.ma@ucsf.edu (A.M.), barbara.malynn@ucsf.edu (B.A.M.)
DOI 10.1016/j.immuni.2010.07.017

SUMMARY

A20 is a ubiquitin modifying enzyme that restricts NF-κB signals and protects cells against tumor necrosis factor (TNF)-induced programmed cell death. Given recent data linking A20 (*TNFAIP3*) with human B cell lymphomas and systemic lupus erythematosus (SLE), we have generated mice bearing a floxed allele of *Tnfaip3* to interrogate A20's roles in regulating B cell functions. A20-deficient B cells are hyperresponsive to multiple stimuli and display exaggerated NF-κB responses to CD40-induced signals. Mice expressing absent or hypomorphic amounts of A20 in B cells possess elevated numbers of germinal center B cells, autoantibodies, and glomerular immunoglobulin deposits. A20-deficient B cells are resistant to Fas-mediated cell death, probably due to increased expression of NF-κB-dependent antiapoptotic proteins such as Bcl-x. These findings show that A20 can restrict B cell survival, whereas A20 protects other cells from TNF-induced cell death. Our studies demonstrate how reduced A20 expression predisposes to autoimmunity.

INTRODUCTION

Maintenance of B cell homeostasis requires proper intracellular integration of signals delivered from multiple surface receptors such as the B cell antigen receptor, Toll-like receptors (TLRs), B cell-activating factor (BAFF) receptor, and CD40, as well as intracellular cues. Failure to integrate pathways such as NF-κB signaling can lead to B cell deficiency, aberrant B cell activity, or even lymphoma. Aberrant B cell tolerance and selection can cause production of autoantibodies, formation of immune complexes (IC), and ultimately tissue damage and autoimmune disease (Fairhurst et al., 2006).

Tnfaip3 encodes the A20 protein, a ubiquitin-modifying enzyme (Wertz et al., 2004; Boone et al., 2004). A20 was initially identified as a TNF-induced molecule that restricts TNF induced signaling (Opipari et al., 1990). Targeting of *Tnfaip3* in mice revealed A20s critical anti-inflammatory functions, given that A20-deficient ($Tnfaip3^{-/-}$) mice exhibit severe spontaneous multiorgan inflammation, cachexia, and perinatal death (Lee et al., 2000). Epistasis experiments revealed that A20 restricts TLR and nucleosome-binding oligomerization domain (NOD) triggered NF-κB signaling, in addition to TNF-induced NF-κB and programmed cell death (PCD) signaling (Lee et al., 2000; Boone et al., 2004; Hitotsumatsu et al., 2008). Thus, A20 restricts a number of innate immune signaling pathways in macrophages and fibroblasts. The severe systemic inflammation and cachexia caused by A20 deficiency is ameliorated in mice that also lack the TLR adaptor protein MyD88 (Turer et al., 2008). Radiation chimeras bearing $Tnfaip3^{-/-}$ hematopoietic cells also develop spontaneous systemic inflammation, which is alleviated by depletion of commensal intestinal bacteria with antibiotics (Turer et al., 2008). Thus, A20 maintains immune homeostasis and restricts the potentially proinflammatory nature of basal MyD88-dependent signals.

In addition to the innate immune functions described above in macrophages and fibroblasts, A20 is also expressed in T and B cells (Sarma et al., 1995; Lee et al., 2000). During T cell activation, A20 is recruited to the MALT-1-Bcl-10 scaffold complex, and is cleaved by the paracaspase MALT-1 (Coornaert et al., 2008). A20 has also been reported to deubiquitinate MALT-1 to restrict TCR signals (Düwel et al., 2009). A20 cleavage is also observed in B lymphoma cell lines in response to BCR stimulation (Coornaert et al., 2008). Other clues that A20 may play important roles in adaptive lymphocytes derives from human genetic studies that implicate A20 (or *TNFAIP3*) as a susceptibility gene for systemic lupus erythematosus (SLE)—an autoimmune disease associated with aberrant B cell function—as well as studies showing that A20 is a tumor suppressor in B cell lymphomas (Graham et al., 2008; Musone et al., 2008; Compagno et al., 2009; Kato et al., 2009; Novak et al., 2009; Schmitz et al., 2009). Nevertheless, the physiological roles of A20 in T and B cells are largely undefined.

B cells are regulated by BCR, TLR, BAFF, and CD40 signals. These signaling cascades share some of the same ubiquitin-dependent signaling molecules utilized by TNF and TLR ligands (e.g., TRAF2, TRAF6, IKKγ) (Hayden and Ghosh, 2008). Given A20's role in preventing inflammation, its genetic linkage to

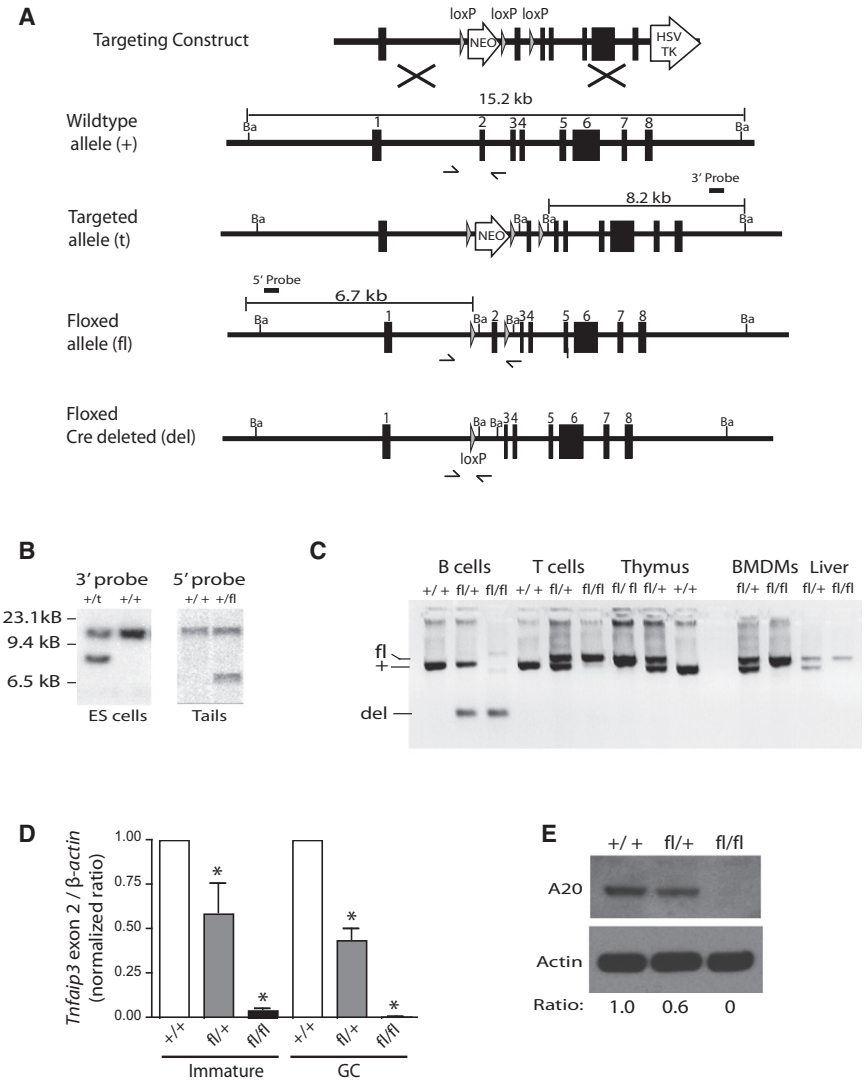

Figure 1. Gene Targeting Strategy to Generate Mice Lacking *Tnfaip3* in B Cells

(A) Schematic representation of the gene targeting construct and screening strategy for obtaining the *Tnfaip3* floxed (fl) allele. Half arrows indicate locations of PCR primers for distinguishing wild-type (+), floxed (fl), and deleted (del) alleles.

(B) Southern blots of BamHI-digested genomic DNA from ESCs showing the targeted allele (left blot) and from tails from mice with germline inheritance of the fl allele (right blot).

(C) Genomic DNA PCR analysis of wild-type (+), floxed (fl), and deleted (del) alleles of *Tnfaip3* exon 2 in the indicated cell types from mice of the indicated genotypes with PCR primers shown in (A). BMDMs are bone marrow-derived macrophages. All mice are *CD19-Cre*$^{+/-}$. PCR products for floxed (fl), wild-type (+), and deleted (del) alleles are indicated. Data are representative of five mice per genotype.

(D) Quantitative genomic DNA PCR analysis of *Tnfaip3* exon 2 in flow cytometry-sorted populations of immature (CD19$^+$ CD93[AA4.1]$^+$) and GC (CD19$^+$ GL7$^+$ CD95$^+$) B cells from mice of the indicated genotypes. PCR primers are described in the Experimental Procedures. Error bars show SEM of three mice per genotype.

(E) Immunoblot analysis of A20 expression in B cells from the indicated genotypes of mice. The A20 to actin protein ratio relative to *Tnfaip3*$^{+/+}$ *CD19-Cre* cells is shown below the blots.

human B cell lymphomas and SLE, and the central role B cells play in SLE pathogenesis, we hypothesized that A20 may regulate B cell homeostasis and prevent autoimmunity. To determine the cell intrinsic functions of A20 in regulating B cells, we have generated mice lacking A20 specifically in these cells.

RESULTS

B-Lineage Deletion of A20 Perturbs Lymphoid Homeostasis

In order to analyze the cell intrinsic functions of A20 in B cells, we generated a targeting construct in which exon 2 of the *Tnfaip3* gene was flanked by loxP sites, a ''floxed'' allele. The targeting construct was transfected into C57BL/6 ES cells and neomycin resistant clones were screened for the targeted allele (Figures 1A and 1B). Transient transfection of Cre recombinase resulted in removal of the neomycin cassette to obtain the floxed *Tnfaip3* allele (Figures 1A and 1B). ES clones were injected into albino C57BL/6 blastocysts, and the resultant chimeras were bred with albino C57BL/6 mice. Non-albino C57BL/6 progeny were screened for the presence of the floxed allele, *Tnfaip3*^{fl} (Figure 1B).

Mice carrying the *Tnfaip3*^{fl} allele were bred with *Cd19-Cre* knock-in mice for generation of *Tnfaip3*$^{+/+}$, *Tnfaip3*$^{fl/+}$ and *Tnfaip3*$^{fl/fl}$ mice bearing a single copy of the *CD19-Cre* allele (Rickert et al., 1997). All mice described in this study were heterozygous for the *CD19-Cre* targeted allele (*CD19-Cre*$^{+/-}$) to control for potential nonspecific effects of Cre expression while maintaining CD19 expression. For simplicity, *CD19-Cre*$^{+/-}$ mice will subsequently be referred to as *CD19-Cre* mice. As has been found for other ''floxed'' alleles, *Tnfaip3*$^{fl/fl}$ *CD19-Cre* mice had efficient and B cell-specific deletion of *Tnfaip3* exon 2, as assessed by genomic polymerase chain reaction (PCR) and Southern blotting (Figure 1C and data not shown). Flow cytometry-sorted immature and germinal center (GC) B cells, subsets represented in smaller proportions, were also nearly 100% deleted as measured by quantitative genomic PCR (Figure 1D). A20 protein is constitutively expressed in B cells and T cells (Figure 1E and data not shown). Deletion of *tnfaip3* exon 2 on both alleles (*Tnfaip3*$^{fl/fl}$ *CD19-Cre*) led to complete loss of A20 protein in splenic B cells (Figure 1E). Note that deletion of one allele of *tnfaip3* in *Tnfaip3*$^{fl/+}$ *CD19-Cre* mice causes hypomorphic (~50%) expression of A20 protein in B cells (Figure 1E).

Tnfaip3$^{fl/fl}$ *CD19-Cre* mice were obtained in Mendelian numbers and developed normally. Hence, these mice differed

Table 1. Cellularity of Lymphoid Organs and Respective Subpopulations in *Tnfaip3*^{fl} *CD19-Cre* Mice

	Tnfaip3$^{+/+}$	*Tnfaip3*$^{fl/+}$	*Tnfaip3*$^{fl/fl}$
Total Cellularity (×10^6)			
Lymph nodes	14.3 ± 0.7	15.8 ± 1.2	25.7 ± 3.7*
Spleen	44.4 ± 11	55.4 ± 9.0	74.2 ± 11
Bone marrow	31.4 ± 3.2	30.7 ± 5.6	31.2 ± 4.1
Peritoneum	4.7 ± 0.7	3.8 ± 1.1	8.1 ± 1.6
Lymph Nodes (×10^6)			
B cells	3.9 ± 0.2	4.7 ± 0.5	8.8 ± 1.1*
T cells	8.9 ± 0.7	8.4 ± 0.8	12.9 ± 1.6*
myeloid cells	0.15 ± 0.03	0.15 ± 0.03	0.24 ± 0.03
mature B cells	2.5 ± 0.1	2.9 ± 0.3	3.3 ± 0.5
immature B cells	1.2 ± 0.1	1.1 ± 0.2	3.9 ± 0.3*
germinal center B cells	0.01 ± 0.003	0.08 ± 0.02*	0.05 ± 0.02*
Spleen (×10^6)			
B cells	23.7 ± 6.0	26.5 ± 4.5	37.8 ± 6.4
T cells	16.5 ± 0.8	16.1 ± 1.7	24.7 ± 2.5*
myeloid cells	0.7 ± 0.03	1.0 ± 0.2	1.4 ± 0.3
mature B cells	11.2 ± 1.4	15.1 ± 3.6	17.9 ± 3.1
immature B cells	9.8 ± 0.6	9.2 ± 0.7	14.8 ± 2.6*
germinal center B cells	0.17 ± 0.03	0.6 ± 0.15*	0.45 ± 0.08*
marginal zone B cells	1.6 ± 0.08	1.1 ± 0.3	0.9 ± 0.2
Peritoneum (×10^6)			
B cells	1.6 ± 0.34	2.7 ± 0.25	4.1 ± 0.37
B1a	0.45 ± 0.04	0.69 ± 0.16	0.6 ± 0.24
B2	0.55 ± 0.16	0.93 ± 0.11	1.6 ± 0.12

Quantitation of lymphoid populations in the indicated tissues from the indicated genotypes of 5- to 7-week-old mice. The total cellularity of lymphoid organs is shown in the top panel. Subpopulations were identified by flow cytometry with the indicated markers: B cells (CD19$^+$); T cells (TCR-β$^+$); myeloid cells (Mac-1$^+$); mature B cells (CD19$^+$, IgM^{Lo}, IgD$^+$); immature B cells (CD19$^+$ IgM^{Hi}); marginal zone B cells (CD21/35^{Hi} CD23^{Lo}); GC B cells (CD19$^+$, GL7$^+$, CD95$^+$); and B1a (IgM$^+$, CD5$^+$). The asterisk indicates significant difference relative to +/+ ($p < 0.05$, with one-way ANOVA). For GC B cells, means are from five mice per genotype; for all other subpopulations, means of 5 *Tnfaip3*$^{+/+}$ *CD19-Cre*, 11 *Tnfaip3*$^{fl/+}$ *CD19-Cre*, and 11 *Tnfaip3*$^{fl/fl}$ *CD19-Cre* mice are shown.

dramatically from mice lacking A20 in all cells or in all hematopoietic cells, both of which develop severe spontaneous inflammation and early lethality (Lee et al., 2000; Boone et al., 2004; Turer et al., 2008). To begin to assess the roles of A20 in regulating B cells, we quantitated lymphoid populations from 5- to 7-week-old *Tnfaip3*$^{fl/fl}$ *CD19-Cre*, *Tnfaip3*$^{fl/+}$ *CD19-Cre* and *Tnfaip3*$^{+/+}$ *CD19-Cre* littermates by flow cytometry (Table 1, top panel). *Tnfaip3*$^{fl/fl}$ *CD19-Cre* mice contained moderately increased numbers of B cells (CD19$^+$), particularly immature B cells (CD19$^+$IgM^{hi}) and germinal center (GC) B cells, when compared to *Tnfaip3*$^{+/+}$ *CD19-Cre* control mice (Table 1, Figures 2A–2C). Although the percentage of B1a (IgM$^+$, CD5$^+$) cells in the peritoneal cavity of *Tnfaip3*$^{fl/fl}$ *CD19-Cre* mice was lower than *Tnfaip3*$^{+/+}$ *CD19-Cre* and *Tnfaip3*$^{fl/+}$ *CD19-Cre* mice, the absolute number was not significantly different (Figure S1A; Table 1). Although A20 deletion in *Tnfaip3*$^{fl/fl}$ *CD19-Cre* mice occurs in B cells and not T cells (Figure 1C), both B cells (CD19$^+$) and T cells (TCR-β$^+$) were modestly expanded in *Tnfaip3*$^{fl/fl}$ *CD19-Cre* mice (Figure 2A and Table 1). The relative percentages of T cell subpopulations (CD4$^+$, CD8$^+$, and T regulatory) were normal (data not shown). Taken together, these findings suggest that A20 restricts the numbers of B cells, particularly immature and GC B cells.

Heterozygous *Tnfaip3*$^{fl/+}$ *CD19-Cre* mice possess largely normal numbers of lymphoid populations, even though *Tnfaip3*$^{fl/+}$ *CD19-Cre* B cells express half the amount of A20 protein as wild-type *Tnfaip3*$^{+/+}$ *CD19-Cre* B cells (Figure 1E). A notable exception is that the numbers of germinal center (GC) (CD95$^+$GL7$^+$) B cells in *Tnfaip3*$^{fl/+}$ *CD19-Cre* mice approximates the number present in *Tnfaip3*$^{fl/fl}$ *CD19-Cre* mice (Figure 2C and Table 1). Thus, proper regulation of GC B cell homeostasis requires more A20 protein than other B cell populations.

Bone marrow from *Tnfaip3*$^{fl/fl}$ *CD19-Cre* and *Tnfaip3*$^{fl/+}$ *CD19-Cre* mice contained normal numbers of B lineage cells, with normal proportions of pro-B (CD43$^+$, IgM$^-$) and pre-B (CD43$^-$, IgM$^-$) cells (Figure S1B). There was a small decrease in the percentage of IgM$^+$ B cells in *Tnfaip3*$^{fl/fl}$ *CD19-Cre* bone marrow, which reflected reductions in mature or recirculating (IgM$^+$, IgD$^+$) B cells (Figure S1B). As CD19 is expressed throughout B cell development, these results suggest that A20 is not required for early B cell differentiation.

The differences in peripheral lymphocyte populations described above persisted but were not further exaggerated in 6-month-old mice (Figure S1C and data not shown). In addition, 6-month-old *Tnfaip3*$^{fl/+}$ *CD19-Cre* and *Tnfaip3*$^{fl/fl}$ *CD19-Cre* mice contained increased percentages of splenic plasma cells when compared to *Tnfaip3*$^{+/+}$ *CD19-Cre* mice (Figure 2D). Whereas markers of B cell activation were expressed normally in 5- to 7-week-old mice, spontaneous B cell activation became apparent in 6-month-old *Tnfaip3*$^{fl/fl}$ *CD19-Cre* but not *Tnfaip3*$^{fl/+}$ *CD19-Cre* mice (Figure 2E and Figure S1D). Spontaneous T cell activation was not observed (data not shown). These findings suggest that A20 expression in B cells prevents spontaneous activation and differentiation of B cells over time.

Overall, elevated numbers of T and B cells and spontaneous B cell activation were observed in *Tnfaip3*$^{fl/fl}$ *CD19-Cre* mice by 6 months of age. In addition, elevated numbers of GC B cells were observed in both heterozygous *Tnfaip3*$^{fl/+}$ *CD19-Cre* mice and homozygous *Tnfaip3*$^{fl/fl}$ *CD19-Cre* mice.

Exaggerated Responses of *Tnfaip3*$^{fl/fl}$ *CD19-Cre* B Cells In Vitro

Our prior work indicated that A20 restricts TNF-, TLR-, and NOD-induced NF-κB signals as well as TNF-induced PCD in fibroblasts and macrophages (Lee et al., 2000; Boone et al., 2004; Hitotsumatsu et al., 2008; Turer et al., 2008). B cells receive activation, proliferation, and survival signals from BCR, CD40 receptor, and other receptors (Skaug et al., 2009). To test whether A20 directly regulates B cell responses, we assayed responses of *Tnfaip3*$^{fl/fl}$ *CD19-Cre*, *Tnfaip3*$^{fl/+}$ *CD19-Cre*, and *Tnfaip3*$^{+/+}$ *CD19-Cre* splenic B cells to LPS, cytosine phosphoguanine oligodeoxynucleotide (CpG) and to agonist anti-IgM and anti-CD40. As noted above, unstimulated splenic B cells from young (5- to 7-week-old) *Tnfaip3*$^{fl/fl}$ *CD19-Cre* mice resembled B cells from *Tnfaip3*$^{fl/+}$ *CD19-Cre* and *Tnfaip3*$^{+/+}$ *CD19-Cre* mice (Figure S1D). *Tnfaip3*$^{fl/fl}$ *CD19-Cre* B cells expressed higher

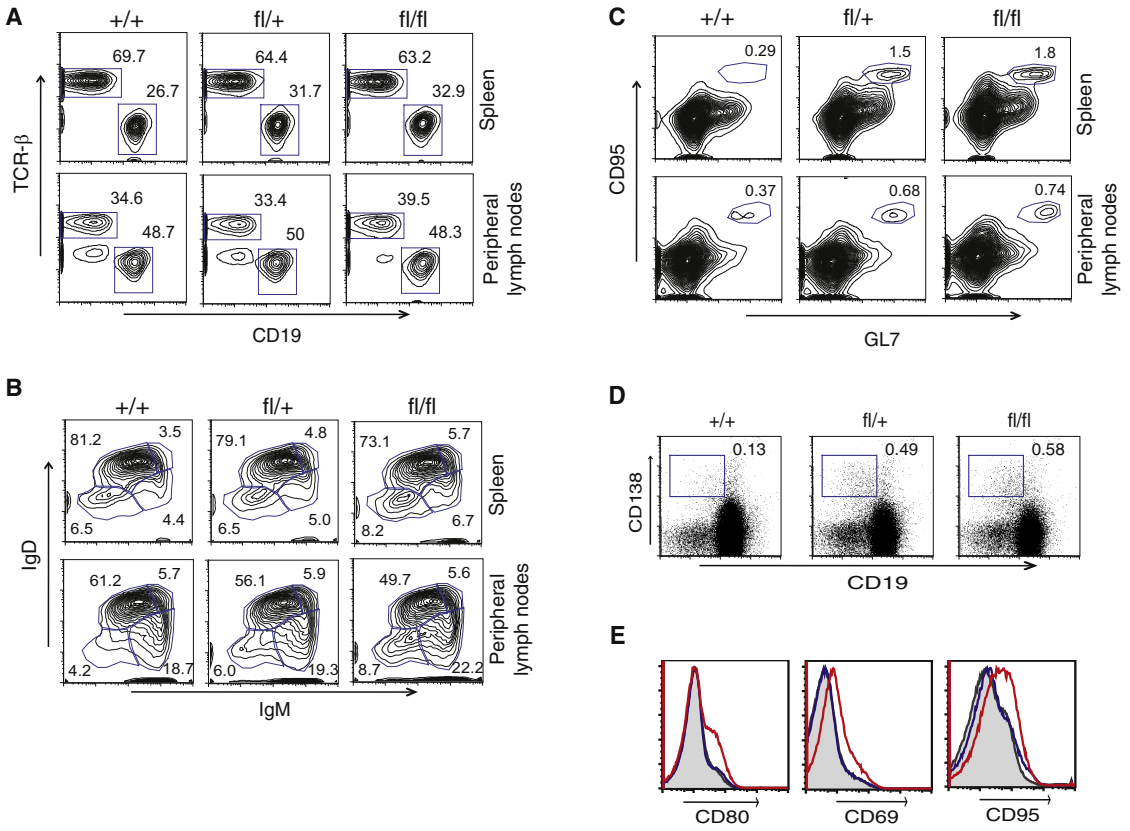

Figure 2. Flow Cytometric Analyses of B Lymphocyte Populations in *Tnfaip3*$^{fl/fl}$ *CD19-Cre* Mice

Flow cytometric analyses of lymphoid tissues.

(A) Analyses of lymphoid populations in spleens and peripheral lymph nodes from 5- to 7-week-old mice.

(B) Analysis of CD19$^+$ gated cells showing B cell maturation (IgM, IgD) from 5- to 7-week-old mice.

(C) Analysis of CD19$^+$ gated cells showing GC B cells (GL7$^+$ CD95$^+$) from 5- to 7-week-old mice.

(D) Plasma cells (CD19$^{+\ low}$ CD138$^+$) within TCR-β$^-$ CD19$^+$ gated splenic B cells from 6-month-old mice are shown. Percentages of cells within the indicated gates are shown on plots (A–D).

(E) Histograms comparing expression of B cell activation markers (CD80, CD69, and CD95) on CD19$^+$ gated B cells from 6-month-old mice: *Tnfaip3*$^{+/+}$ (shaded histogram), *Tnfaip3*$^{fl/+}$ (blue line), and *Tnfaip3*$^{fl/fl}$ (red line). All data compare littermates of the indicated genotypes and are representative of three to five mice per genotype.

amounts of CD80 (B7.1) and CD69 after stimulation with several B cell agonists (Figure 3 and data not shown). *Tnfaip3*$^{fl/fl}$ *CD19-Cre* B cells also proliferated to a greater extent than control cells (Figure 3B). Third, *Tnfaip3*$^{fl/fl}$ *CD19-Cre* B cells produced more IL-6 than *Tnfaip3*$^{fl/+}$ *CD19-Cre* and *Tnfaip3*$^{+/+}$ *CD19-Cre* cells after treatment with LPS and CpG (Figure 3C).

To control for potential differences in B cell populations and to avoid potential caveats associated with developmental abnormalities, we sought to eliminate A20 expression in mature B cells after B cell development. Accordingly, we interbred *Tnfaip3*^{fl} mice with estrogen receptor (ER)-Cre [Gt(ROSA)26ER-Cre] mice to obtain mice in which A20 (*Tnfaip3*) deletion would not occur until cells were exposed to 4-hydroxytamoxifen (4-OH-T). Splenic B cells enriched from *Tnfaip3*$^{fl/fl}$ ER-Cre mice and treated with 4-OH-T in vitro effectively ablated A20 protein expression (Figure 3D). We then tested responses of these B cells. Consistent with our findings with *Tnfaip3*$^{fl/fl}$ *CD19-Cre* B cells, mature splenic *Tnfaip3*$^{fl/fl}$ ER-Cre B cells rendered acutely A20 deficient with 4-OH-T exhibited exaggerated responses to all receptor stimuli when compared to control *Tnfaip3*$^{fl/+}$ ER-Cre cells (Figure 3E). Thus, A20 expression in mature B cells restricts B cell responses independently of any potential roles of A20 in regulating B cell development.

A20 Restricts NF-κB Activation Signals Downstream of CD40

A20 restricts cellular responses to TNF, TLR, and NOD2 ligands by restricting NF-κB signaling (Lee et al., 2000; Boone et al., 2004; Hitotsumatsu et al., 2008; Turer et al., 2008). CD40 is a tumor necrosis factor receptor (TNFR) family member that triggers NF-κB signals and supports B cell activation and survival (Elgueta et al., 2009). To test whether A20 directly restricts CD40-induced NF-κB signals, we stimulated splenic B cells from *Tnfaip3*$^{+/+}$ *CD19-Cre* and *Tnfaip3*$^{fl/fl}$ *CD19-Cre* mice with agonist anti-CD40 antibody. A20 protein was dramatically induced by CD40 engagement in *Tnfaip3*$^{+/+}$ *CD19-Cre* B cells, whereas no A20 expression was observed in *Tnfaip3*$^{fl/fl}$ *CD19-Cre* B cells (Figure 4). *Tnfaip3*$^{fl/fl}$ *CD19-Cre* B cells displayed

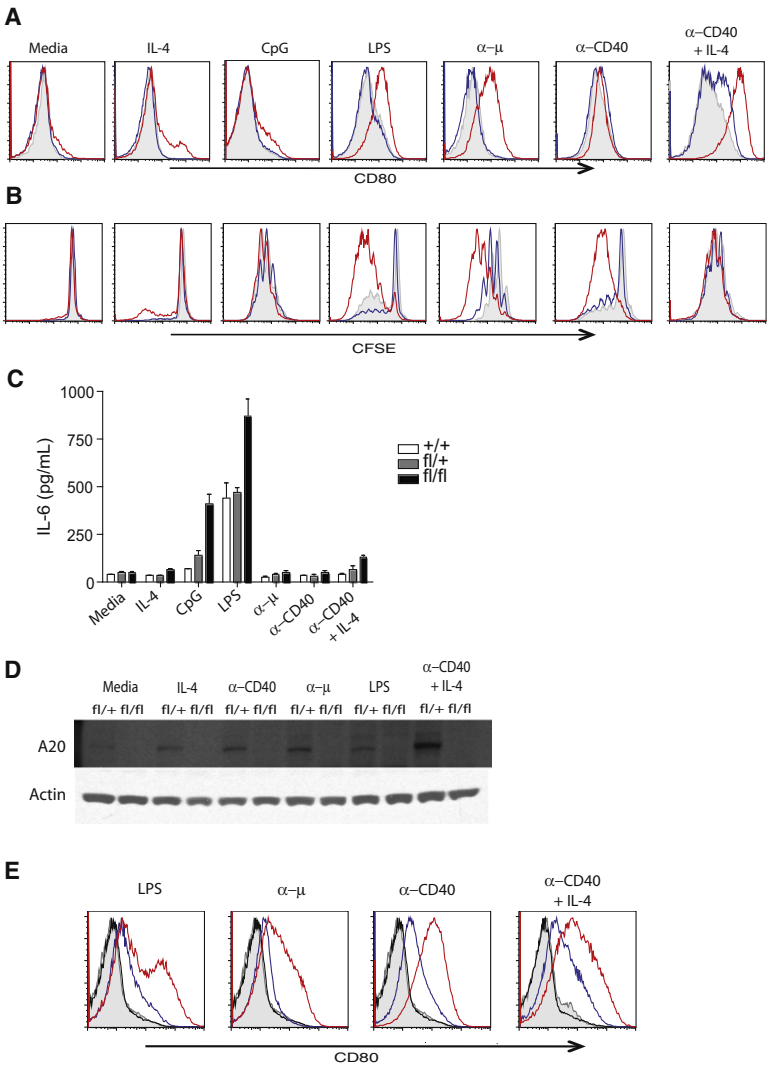

Figure 3. Hyperresponsiveness of A20-Deficient B Cells

In vitro responses of purified B cells after stimulation with the indicated stimuli for 72 hr. Flow cytometric analyses of (A) surface expression of the activation marker CD80 (B7.1) and (B) dilution of CFSE-labeled cells. *Tnfaip3*$^{fl/fl}$ *CD19-Cre* (red lines), *Tnfaip3*$^{fl/+}$ *CD19-Cre* (blue lines), and *Tnfaip3*$^{+/+}$ *CD19-Cre* (shaded gray) histograms are shown. In (C), ELISA determination of IL-6 secretion in the supernatants of 72 hr B cell cultures is shown. Means and standard deviations (SD) of triplicate wells are shown. (D) shows immunoblots of A20 and actin protein expression in purified Rosa-ER-Cre^{+} B cells of the indicated genotypes. Lysates were isolated after 72 hr stimulation with the indicated ligands in the presence of 4-OH-T. As shown in (E), expression of CD80 in purified B cells after treatment with 4-OH-T and the indicated ligands for 72 hr. *Tnfaip3*$^{fl/fl}$ GT-Rosa-Cre^{+} B cells treated with IL-4 or media (black lines) or the indicated ligands (red lines) and *Tnfaip3*$^{fl/+}$ GT-Rosa-Cre^{+} B cells treated with IL-4 or media (gray shaded histograms) or the indicated ligands (blue lines) are shown. All data are representative of three independent experiments.

increased and prolonged canonical NF-κB signaling as measured by IκBα phosphorylation in response to anti-CD40 (Figure 4B). Agonist anti-CD40 also induced greater amounts of phospho-p100, an indicator of noncanonical NF-κB signaling, in *Tnfaip3*$^{fl/fl}$ *CD19-Cre* B cells when compared to *Tnfaip3*$^{+/+}$ *CD19-Cre* B cells (Figure 4C). This increased noncanonical NF-κB signaling correlates with increased basal p100 protein amounts in *Tnfaip3*$^{fl/fl}$ *CD19-Cre* B cells (Figure 4C). By contrast, Erk phosphorylation was similarly induced in *Tnfaip3*$^{fl/fl}$ *CD19-Cre* and control B cells (Figure 4D).

Normal Antigen-Specific B Cell Responses in *Tnfaip3*$^{fl/fl}$ *CD19-Cre* Mice

A20s capacity to restrict B cell activation in vitro suggests that *Tnfaip3*$^{fl/fl}$ *CD19-Cre* mice might exhibit exaggerated antigen-specific B cell responses in vivo. We thus tested antigen-specific B cell responses to NP-KLH in these mice. At baseline, *Tnfaip3*$^{fl/fl}$ *CD19-Cre* mice have more IgM and modestly elevated amounts of IgGs (Figure S2A). *Tnfaip3*$^{fl/fl}$ *CD19-Cre* mice produced proportionately higher amount of anti-NP IgM antibodies before and after immunization with NP-KLH (Figure S2B). All genotypes of mice generated similar amounts of anti-NP IgG (Figure S2C). Thus, T cell-dependent B cell responses occur largely normally in *Tnfaip3*$^{fl/fl}$ *CD19-Cre* mice. Anti-NP-Ficoll IgM responses paralleled T cell dependent NP-KLH responses in *Tnfaip3*$^{fl/fl}$ *CD19-Cre* mice, indicating that T cell-independent B cell responses also occur normally in these mice (data not shown).

Tnfaip3$^{fl/fl}$ *CD19-Cre* and *Tnfaip3*$^{fl/+}$ *CD19-Cre* Mice Develop Autoimmunity

Increased numbers of immature and germinal center B cells suggest that autoreactive B cells may accumulate and produce autoantibodies in *Tnfaip3*$^{fl/fl}$ *CD19-Cre* mice. In addition, several SNPs near the human A20 (*TNFAIP3*) gene are independently associated with susceptibility to SLE (Graham et al., 2008; Musone et al., 2008). To characterize the autoantibody profile of *Tnfaip3*$^{fl/+}$ *CD19-Cre* mice and *Tnfaip3*$^{fl/fl}$ *CD19-Cre* mice as compared to *Tnfaip3*$^{+/+}$ *CD19-Cre* mice, we used large-scale 1152 feature protein and peptide microarrays to detect autoantibodies directed against over 140 antigens (Robinson et al., 2002). Antibodies to over 46 self-antigens were detected, including antibodies to nuclear antigens (e.g., single-stranded DNA, small ribonuclear proteins A and C, and Ku protein), glomerular antigens (e.g., vimentin, collagen X, proteoglycan, and aggrecan), and heat-shock proteins (Figure 5A). Importantly, the serum autoantibody profiles from *Tnfaip3*$^{fl/fl}$ *CD19-Cre* and *Tnfaip3*$^{fl/+}$ *CD19-Cre* mice clustered well with each other and away from *Tnfaip3*$^{+/+}$ *CD19-Cre* mice (Figure 5A). These autoantibodies were observed in both male and female mice and were observed in C57BL/6 inbred mice, a strain that is relatively resistant to SLE-like disease. Elispot analysis for anti-DNA indicate both an increase in the number and size of anti-DNA producing B cells in *Tnfaip3*$^{fl/fl}$ *CD19-Cre* mice (Figure 5B and data not shown). These findings indicate that

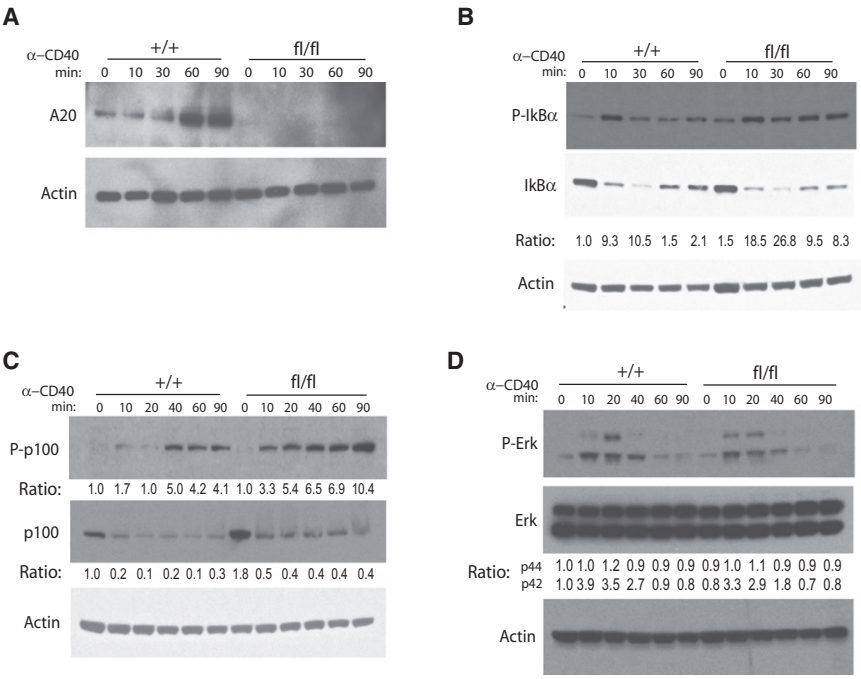

Figure 4. A20 Restricts NF-κB Signaling Downstream of CD40 Signals

(A) Immunoblot analysis of A20 protein induction by agonist anti-CD40.

(B) Immunoblot analyses of phospho-IκBα and IκBα after CD40 stimulation. Ratios of pIkBα/IkBα were normalized to time 0 of *Tnfaip3*$^{+/+}$ *CD19-Cre* cells and are shown below.

(C) Immunoblot analyses of NF-κB P-p100 (upper panel) and p100 (middle panel) protein amounts in response to agonist CD40 antibody. Ratios of P-p100/actin, normalized to time 0 sample in *Tnfaip3*$^{+/+}$ *CD19-Cre* B cells, are shown below P-p100 immunoblot. Ratios of p100/actin, normalized to time 0 sample in *Tnfaip3*$^{+/+}$ *CD19-Cre* B cells, are shown below p100 immunoblot.

(D) Immunoblot analysis of Erk signaling. Ratios of pErk/Erk were normalized to time 0 of *Tnfaip3*$^{+/+}$ *CD19-Cre* cells and are shown below. Actin protein amounts shown below all panels as loading controls. Data are representative of three independent experiments.

A20 expression in B cells prevents spontaneous production of autoantibodies.

Autoantibodies can be deposited in glomeruli of kidneys of SLE patients and ultimately cause glomerulonephritis. To determine whether serum autoantibodies in *Tnfaip3*$^{fl/fl}$ *CD19-Cre* and *Tnfaip3*$^{fl/+}$ *CD19-Cre* mice lead to glomerular Ig deposits, we examined kidneys from 6-month-old mice by histology and immunofluorescence. Although kidney sections appeared histologically normal, IgM deposits were observed in the kidneys of both *Tnfaip3*$^{fl/fl}$ *CD19-Cre* and *Tnfaip3*$^{fl/+}$ *CD19-Cre* mice (Figure 5C). IgG deposits were more prominent in *Tnfaip3*$^{fl/+}$ *CD19-Cre* mice (Figure 5C).

In addition to autoantibody-producing B cells "escaping" from negative selection, activation of innate immune cells and type I interferon (IFN I) secretion may be key factors contributing to autoantibody production and the pathogenesis of SLE (Fairhurst et al., 2006; Shlomchik, 2008). CpG triggers B cell activation and production of type I interferons (IFNs), and increases class switching to pathogenic autoantibody isotypes (Ehlers et al., 2006). We thus asked whether *Tnfaip3*$^{fl/+}$ *CD19-Cre* and *Tnfaip3*$^{fl/fl}$ *CD19-Cre* mice develop more autoimmune disease after stimulation with CpG. CpG treatment of intact mice enhanced production of IgG dsDNA antibodies in serum as well as pathogenic deposition of IgG in renal glomeruli of both *Tnfaip3*$^{fl/fl}$ *CD19-Cre* and *Tnfaip3*$^{fl/+}$ *CD19-Cre* mice but not *Tnfaip3*$^{+/+}$ *CD19-Cre* mice (Figure 5D and data not shown). Taken together, these findings indicate that A20 expression in B cells prevents autoimmunity.

A20 Restricts B Cell Survival to Fas-Mediated PCD

Tnfaip3$^{fl/+}$ *CD19-Cre* mice share two key features with *Tnfaip3*$^{fl/fl}$ *CD19-Cre* mice: increased numbers of GC B cells and susceptibility to autoimmunity. These observations suggest that the amount of A20 expression regulates B cell selection in germinal centers. One possible mechanism for negative selection of autoreactive B cells in GCs is Fas-induced PCD (Hao et al., 2008). We thus tested the susceptibility of *Tnfaip3*$^{+/+}$ *CD19-Cre*, *Tnfaip3*$^{fl/+}$ *CD19-Cre*, and *Tnfaip3*$^{fl/fl}$ *CD19-Cre* B cells to Fas-induced PCD. Splenic B cells were activated with agonist anti-CD40 to induce Fas sensitivity. As expected, activation of *Tnfaip3*$^{+/+}$ *CD19-Cre* B cells caused increased expression of Fas and dose-dependent sensitivity to Fas-mediated PCD (Figures 6A and 6B). *Tnfaip3*$^{fl/fl}$ *CD19-Cre* B cells expressed higher amounts of surface Fas than *Tnfaip3*$^{+/+}$ *CD19-Cre* B cells after CD40 stimulation, while *Tnfaip3*$^{fl/+}$ *CD19-Cre* B cells expressed intermediate amounts (Figure 6A). Remarkably, *Tnfaip3*$^{fl/fl}$ *CD19-Cre* and *Tnfaip3*$^{fl/+}$ *CD19-Cre* B cells were resistant to Fas-mediated PCD when compared to control *Tnfaip3*$^{+/+}$ *CD19-Cre* cells—even though *Tnfaip3*$^{fl/fl}$ *CD19-Cre* and *Tnfaip3*$^{fl/+}$ *CD19-Cre* B cells expressed greater amounts of Fas (Figure 6B). This finding is particularly surprising given our prior observation that A20-deficient fibroblasts are more susceptible to TNF-induced PCD than normal cells (Lee et al., 2000). Thus, A20 supports Fas-mediated PCD in B cells and inhibits TNFR-induced PCD in fibroblasts.

To understand why A20-deficient B cells are resistant to Fas mediated PCD, we hypothesized that increased NF-κB signaling in these cells might lead to increased expression of anti-apoptotic proteins such as Bcl-x. After stimulation with agonist anti-CD40 in vitro, *Bcl-x* mRNA expression increased within 1 hr and rose to a higher amount in *Tnfaip3*$^{fl/fl}$ *CD19-Cre* B cells compared with *Tnfaip3*$^{fl/+}$ *CD19-Cre* or *Tnfaip3*$^{+/+}$ *CD19-Cre* B cells (Figure 6C). CD40 triggered induction of Bcl-x mRNA was blocked by the NF-κB inhibitor, NEMO-binding domain (NBD) peptide, but not by control peptide (Figure 6C). Hence, NF-κB signaling appears directly required for induced Bcl-x mRNA

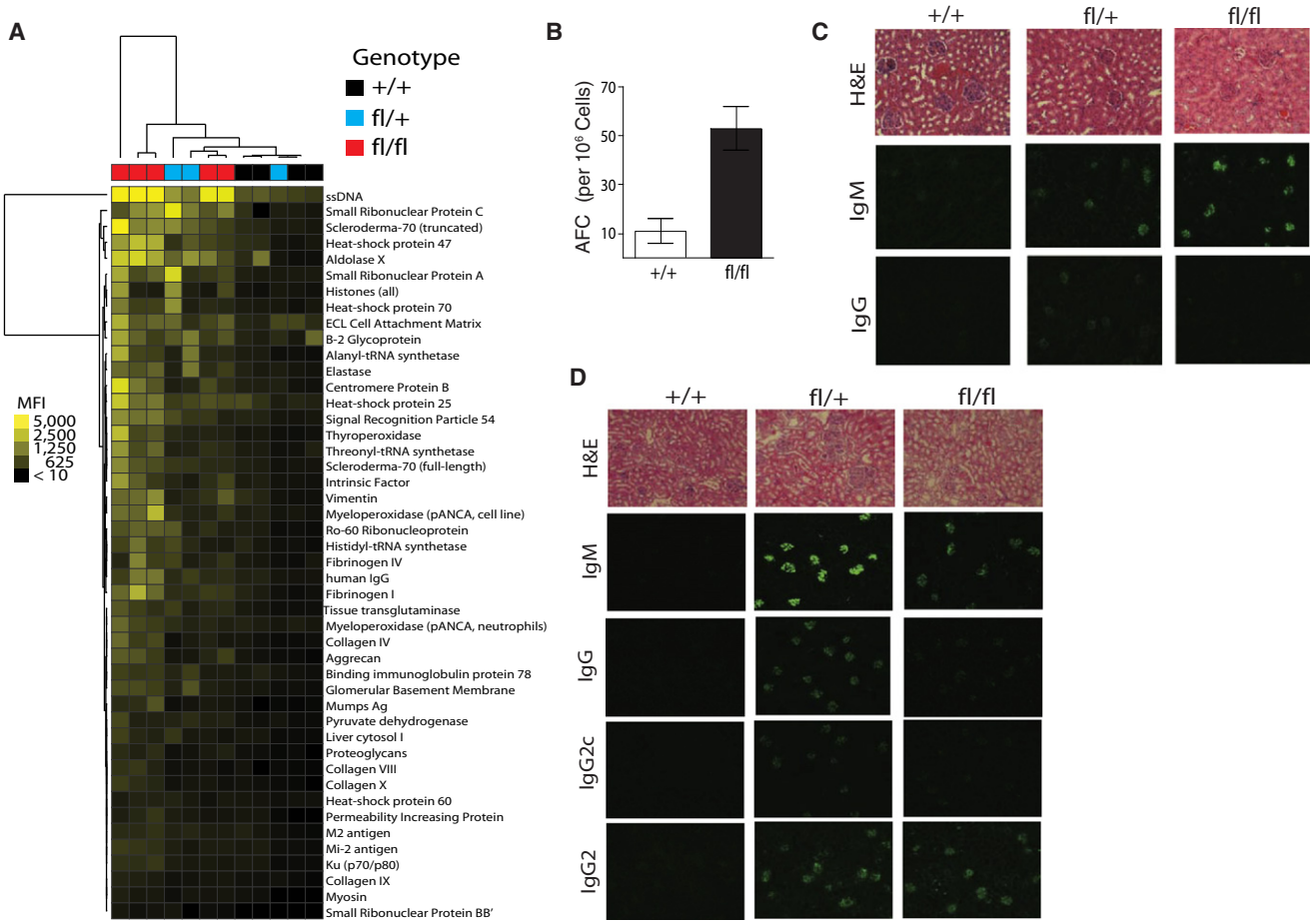

Figure 5. Spontaneous Autoantibody Production in *Tnfaip3*$^{fl/+}$ *CD19-Cre* and *Tnfaip3*$^{fl/fl}$ *CD19-Cre* Mice

(A) Protein array analyses of autoantibodies in sera from 3 month old *Tnfaip3*$^{fl/fl}$ *CD19-Cre* (n = 5), *Tnfaip3*$^{fl/+}$ *CD19-Cre* (n = 3), and *Tnfaip3*$^{+/+}$ *CD19-Cre* (n = 4) mice. Heat map shows relative reactivity to the respective antigens on the arrays, hierarchically clustered in both axes by Euclidean distance. The reactivity intensities (MFI) are depicted on a relative color scale. Statistically different antigens were identified with two-class significant analysis of microarrays (SAMs) with an unpaired t test.

(B) Antibody-forming cells (AFCs) measured by Elispot for anti-dsDNA Ig-producing B cells. Counts were plotted as the mean of triplicate wells and SD is shown. Data are representative of three independent experiments.

(C) Immunofluorescent analyses of glomerular Ig deposition in 6-month-old mice of indicated genotypes. Analyses of IgM and IgG deposits shown in upper and middle panels, respectively. Data are representative of at least three mice per genotype.

(D) Immunofluorescent analyses of glomerular deposition of Igs of the indicated isotypes after CpG treatment. Eight to ten-week-old mice (n = 4) of the indicated genotypes were treated with 40 μg of CpG intraperitoneally every other day for 2 weeks. Mice were analyzed 6 weeks after start of treatment. Hematoxlin and eosin (H&E) sections are shown above, and all sections are shown at 100× the original magnification (C and D).

transcription. Consistent with enhanced Bcl-x mRNA expression, markedly higher quantities of Bcl-x protein appear in *Tnfaip3*$^{fl/fl}$ *CD19-Cre* B cells compared with *Tnfaip3*$^{fl/+}$ *CD19-Cre* or *Tnfaip3*$^{+/+}$ *CD19-Cre* B cells (Figure 6D). Taken together, these findings indicate that A20 restricts the survival of activated B cells by limiting the NF-κB-dependent transcription of Bcl-x mRNA and the subsequent production of Bcl-x protein. They also provide a potential mechanism by which A20 deficient B cells are resistant to negative selection in germinal centers.

DISCUSSION

The generation and characterization of mice lacking A20 specifically in B cells, *Tnfaip3*$^{fl/fl}$ *CD19-Cre* mice, has allowed us to unveil several functions for A20. We have discovered that B cell-specific expression of A20 restricts CD40 and BCR responses, terminates CD40-triggered NF-κB signals, restricts B cell survival, and prevents autoimmunity. These studies provide unique molecular insights into B cell homeostasis, human SLE and B cell lymphomas.

Tnfaip3$^{fl/fl}$ *CD19-Cre* mice are largely healthy, in marked contrast to mice lacking A20 expression in all cells or in all hematopoietic cells. This observation is consistent with our prior suggestion that the cachexia, myeloid dysregulation, and perinatal lethality observed in globally A20-deficient mice is largely due to myeloid cell dysfunction. Although *Tnfaip3*$^{fl/fl}$ *CD19-Cre* mice contained mild expansion of T cell numbers, these perturbations are probably not due to aberrant A20 deletion as judged

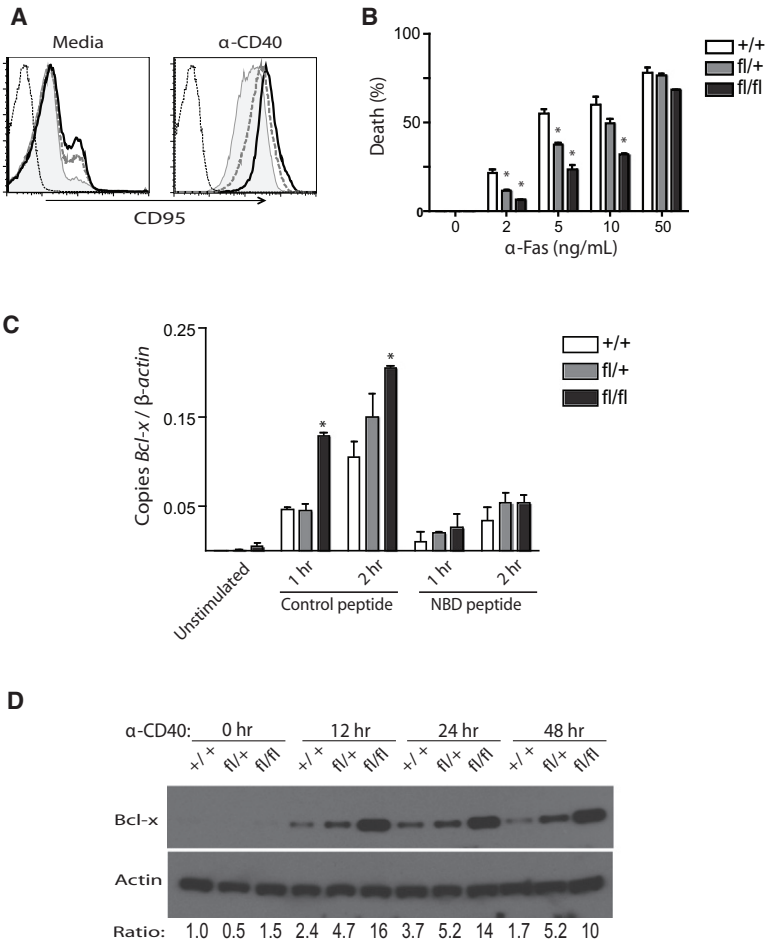

Figure 6. A20-Deficient and Hypomorphic B Cells Are Resistant to Programmed Cell Death

(A) Flow cytometric analyses of CD95 (Fas) expression in enriched B cells after agonist anti-CD40 stimulation. Overlays of CD95 histograms on gated CD19$^+$ cells from *Tnfaip3*$^{+/+}$ *CD19-Cre* (shaded), *Tnfaip3*$^{fl/+}$ *CD19-Cre* (dashed line), *Tnfaip3*$^{fl/fl}$ *CD19-Cre* (black line), and unstained control (dotted line) are shown.

(B) Enriched B cells stimulated for 48 hr with agonist anti-CD40 and treated with the indicated concentrations of agonist anti-CD95 for 12 hr were analyzed for survival by measuring the percentage of dead (Annexin-V$^+$ DAPI$^+$) cells by flow cytometry. Percent death was calculated as ([% Fas-induced dead − % control dead]/[100% − % control dead]). Data are plotted as mean ± SD of triplicate wells. The asterisk indicates $p < 0.001$ with two-way ANOVA. The asterisk indicates $p < 0.05$ in comparison with +/+ samples by Student's t test.

(C) Bcl-x mRNA amounts measured by real-time quantitative (RT qPCR) in enriched B cells. Cells of the indicated genotypes were stimulated with agonist anti-CD40 for the indicated times in the presence of an inhibitor (NBD) or a control peptide, or left unstimulated. Data are plotted as mean ± SD of triplicate wells. $p < 0.001$ with two-way ANOVA; the asterisk indicates $p < 0.05$ in comparison with +/+ samples by Student's t test.

(D) Immunoblot analysis for the expression of Bcl-x protein in B cells of the indicated genotypes stimulated with agonist anti-CD40 for the indicated times. Actin protein amounts are shown below as a control. Ratios of Bcl-x to actin protein, normalized to the *Tnfaip3*$^{+/+}$ B cells at time 0, are shown below each sample. All data are representative of three independent experiments.

by our molecular analyses and by the published literature for this Cre strain (Rickert et al., 1997; Schmidt-Supprian and Rajewsky, 2007). Rather, these mice express increased quantities of splenic IL-4 mRNA (data not shown), and *Tnfaip3*$^{fl/fl}$ *CD19-Cre* B cells produced more IL-6 and expressed higher amounts of costimulatory molecules upon stimulation. Thus, T cell expansion may be due to antigen-independent bystander effects induced by B cell-derived cytokines and/or costimulatory molecules, as has been observed in other settings of B cell hyperresponsiveness (Hömig-Hölzel et al., 2008; Hao et al., 2008).

Our findings demonstrate that A20 performs important functions in adaptive immune cells in addition to previously described functions in innate immune cells (Lee et al., 2000; Boone et al., 2004; Hitotsumatsu et al., 2008). A20's roles in restricting CD40- and BCR-triggered NF-κB signals add to the spectrum of signaling cascades regulated by this ubiquitin modifying enzyme. NF-κB signaling is important for regulating B cell homeostasis (Sen, 2006; Siebenlist et al., 2005). The phenotypes of our mice lacking A20 expression in B cells reveal the importance of tightly regulating basal NF-κB signals in these cells.

B cell-specific loss of A20 expression leads to increased numbers of autoantibody-producing cells. B cells undergo several stages of negative selection to eliminate autoreactive cells both in the bone marrow and in peripheral lymphoid organs (Jacobi and Diamond, 2005; Shlomchik, 2008; Yurasov and Nussenzweig, 2007; von Boehmer and Melchers, 2010). In the bone marrow, immature B cells are selected as a consequence of BCR and BAFF signals and intracellular cell survival factors. In the periphery, selection occurs during GC maturation. Germinal centers are sites where B cells undergo expansion, immunoglobulin class switching, somatic hypermutation, and affinity maturation (Klein and Dalla-Favera, 2008). B cells with low affinity for antigen or reactivity for self-antigens are negatively selected within GCs (Shlomchik, 2008). Deletion of autoreactive B cells helps prevent autoimmunity, and defective GC selection of autoreactive B cells has been observed in human SLE patients (Cappione et al., 2005). Fas (CD95) is highly expressed on GC B cells (Watanabe et al., 1995). Although the role of Fas-mediated PCD in GC selection has been controversial (Smith et al., 1995; Takahashi et al., 2001; Mizuno et al., 2003; Hao et al., 2008), Fas mediated PCD likely plays an important role in eliminating autoreactive B cells (Rathmell et al., 1995; Fukuyama et al., 2002; William et al., 2002). Thus, the accumulation of GC B cells in *Tnfaip3*$^{fl/+}$ *CD19-Cre* and *Tnfaip3*$^{fl/fl}$ *CD19-Cre* mice may be due to the increased resistance of A20-deficient B cells to physiological PCD, leading to the escape of autoreactive B cells.

How might A20 deficiency in B cells render them resistant to PCD? One possibility stems from the observation that NF-κB-dependent proteins protect B cells against PCD. Indeed, both canonical and noncanonical NF-κB signaling downstream of BCR, CD40, BAFF, and TLR receptors are thought to promote B cell survival as well as proliferation and activation (Siebenlist

et al., 2005; Sen, 2006; Hömig-Hölzel et al., 2008). NF-κB has been suggested to be necessary for mediating BCR-induced resistance to Fas-mediated PCD (Mizuno et al., 2003; Schram and Rothstein, 2003). Our studies indicate that A20 directly restricts canonical NF-κB signals and suggest that these signals may lead to elevated noncanonical NF-κB signals. These increased NF-κB signals lead to increased expression of antiapoptotic proteins such as Bcl-2 and Bcl-x. Deregulated expression of these proteins has been shown to cause altered GC B cell selection (Grillot et al., 1996; Takahashi et al., 1999). Hence, increased expression of Bcl-x and/or other NF-κB-dependent proteins may provide a molecular underpinning for increased numbers of GC B cells in *Tnfaip3*$^{fl/fl}$ *CD19-Cre* mice.

Heterozygous *Tnfaip3*$^{fl/+}$ *CD19-Cre* mice contain similarly increased numbers of GC B cells and autoantibodies as homozygous *Tnfaip3*$^{fl/fl}$ *CD19-Cre* mice at young ages (i.e., 5–7 weeks old), suggesting that a high threshold of A20 expression must be maintained for properly selecting (or deleting) these cells. Reduced A20 expression in other cell types leads to increased production of NF-κB-dependent gene products, so endogenous amounts of A20 protein appear to be limiting (A.M., unpublished data). Reduced (rather than absent) quantities of A20 expression or hypomorphic A20 proteins may also link A20 (*TNFAIP3*) susceptibility SNPs with SLE in human patients (Musone et al., 2008). Thus, mice expressing reduced amounts of A20 may prove to be highly relevant models of human autoimmune diseases.

Although reduced A20 expression in B cells leads to accumulation of GC B cells and IgG autoantibodies, absent A20 expression also causes accumulation of immature B cells and IgM in *Tnfaip3*$^{fl/fl}$ *CD19-Cre* mice and progressive activation of B cells with age. Hence, a lower amount of A20 is necessary to preserve selection of immature B cells and to restrict spontaneous B cell activation than the amount required for proper GC selection. As IgM autoantibodies may be protective against IgG-mediated autoimmune disease, higher IgM amounts in homozygous *Tnfaip3*$^{fl/fl}$ *CD19-Cre* mice may reduce the degree of autoimmune disease observed in these mice (Witte, 2008). A20 amounts are dynamically regulated, largely in response to NF-κB signals (Krikos et al., 1992). Thus, A20 expression amounts appear to be finely tuned to regulate NF-κB signaling and survival of distinct subsets of B cells.

Tnfaip3$^{fl/fl}$ *CD19-Cre* mice exhibit largely normal antigen specific B cell responses in vivo, despite the fact that mature *Tnfaip3*$^{fl/fl}$ *CD19-Cre* B cells exhibit increased responses to BCR, CD40, and TLR ligands in vitro. These findings suggest that B cell-independent factors such as T cells and myeloid cells can properly restrict antigen-specific B cell responses, even if they allow progressive accumulation of autoreactive B cells in *Tnfaip3*$^{fl/fl}$ *CD19-Cre* mice.

Our experiments indicate that A20 expression in B cells regulates GC B cell selection as well as B cell activation, thereby regulating key aspects of B cell tolerance. It is remarkable that B cell-specific deletion of A20 alone is sufficient for autoimmunity in C57BL/6 mice. The appearance of IgG deposits suggests that abnormal B cells are sufficient for at least the initial stages of the autoimmunity and are part of the continuum to full-blown disease. Hence, lupus-prone *Tnfaip3*$^{fl/fl}$ *CD19-Cre* and *Tnfaip3*$^{fl/+}$ *CD19-Cre* mice as well as genetic derivatives of these mice should be useful models for understanding human SLE. Heterozygous *Tnfaip3*$^{fl/+}$ *CD19-Cre* mice may be particularly relevant, as reduced, rather than absent A20 expression may characterize this human condition.

Recent studies have shown that somatic loss of A20 in B cells causes several types of Hodgkin, non-Hodgkin, and marginal zone B cell lymphomas in humans (Kato et al., 2009; Compagno et al., 2009; Schmitz et al., 2009; Novak et al., 2009). Our findings that A20-deficient B cells express high amounts of Bcl-x and are resistant to Fas-mediated PCD provide molecular insights into how A20 functions as a tumor suppressor in B cells. Remarkably, A20 is a proapoptotic protein in B cells even though it restricts TNF-induced apoptosis in fibroblasts and hepatocytes (Lee et al., 2000; Arvelo et al., 2002). Hence, it is critical to analyze A20's physiological functions in cell type-specific contexts. Future studies testing the potential of A20 deficiency to collaborate with other B cell oncogenes may reveal the spectrum of A20's tumor suppressor functions in B cells.

In conclusion, we have demonstrated functions for A20 in regulating B cell responses, including the restriction of CD40-induced NF-κB signals. These cell-autonomous functions are critical for B cell homeostasis and the prevention of autoreactive B cells and autoimmunity. In addition to unveiling new molecular mechanisms of B cell homeostasis, these studies provide critical insights into the pathogenesis of human SLE and B cell lymphomas.

EXPERIMENTAL PROCEDURES

Generation of A20 Conditionally Targeted (*Tnfaip3*$^{fl/fl}$) Mice

Recombineering was used for generating a gene targeting construct from a bacterial artificial chromosome (BAC) from the C57BL/6J strain containing the *tnfaip3* gene. C57BL/6 ESCs (PRX-B6T, Primogenix) were transfected with this construct, and successfully targeted ESCs were identified by Southern blot analysis. Correctly targeted clones were then transfected with recombinant Cre and screened for removal of the neomycin cassette for obtaining the *tnfaip3* "floxed" allele. Blastocyst injections of targeted ESCs were performed by the UCSF Transgenic Core. Chimeras were bred to albino C57BL/6J mice and nonalbino progeny were screened for the presence of the floxed allele (*Tnfaip3*$^{fl/+}$). Mice bearing the targeted allele in the germline were interbred with *CD19-Cre* mice on the C57BL/6 background (B6.129P2(C)-CD19$^{tm1(cre)Cgn}$/J) (Rickert et al., 1997). *Tnfaip3*$^{fl/fl}$ or *Tnfaip3* $^{fl/+}$ mice homozygous for *CD19-Cre* were bred with *Tnfaip3*$^{fl/fl}$ or *Tnfaip3* $^{fl/+}$ mice without the *CD19-Cre* allele for generating experimental mice of various *Tnfaip3* genotypes (*Tnfaip3*$^{+/+}$, *Tnfaip3*$^{fl/+}$ and *Tnfaip3*$^{fl/fl}$) that have one copy of Cre and are heterozygous for CD19. Genotypes were initially confirmed by Southern blot analysis and subsequently identified by PCR with the following primers: 5′-AACTTTACAGTCCCCAGCAATGG-3′ (sense); and 5′-GAGGAGGTTGGAA GACATAGAATCG-3′ (antisense).

Cell Preparation and Analyses

Single-cell suspensions were prepared and incubated with the designated conjugated antibodies (all from BD Biosciences, except anti-CD5 and anti-CD93 [AA4.1], eBioscience), and live cells (DAPI^{-}) were analyzed by flow cytometry (LSRII, BD Biosciences) with FlowJo software (Tree Star). BMDMs were prepared as previously described (Boone et al., 2004). For in vitro assays, B cells were isolated by negative depletion with TCRβ, Mac-1, NK1.1 and Ter119 biotinylated antibodies (BD Biosciences) bound to streptavidin coated magnetic beads (M-280 Dynabeads, Invitrogen). Cells were stimulated with anti-CD40 (HM40-3, BD Biosciences) at 1 μg/ml, anti-μ chain (Jackson Immunoresearch) at 2 μg/ml, IL-4 (Peprotech) at 10 ng/ml, and LPS (Sigma) at 1 μg/ml. For in vitro deletion of *tnfaip3* exon 2 from GT-Rosa Cre B cells, cells were treated with 4-OH-T (2.5 nM) for the first 12 hr of stimulation. For NF-κB inhibition, control peptide or NBD Peptide (Calbiochem) was added at 0.5 μM 1 hr prior to stimulation with agonist CD40 antibody.

Mouse Immunizations

For in vivo antigen responses, 6- to 8-week-old mice were injected intraperitoneally (i.p.) and bled on the indicated days. Mice were injected with 50 μg NP-KLH (Biosearch Technologies) mixed 1:1 with Imject Alum (Thermo Scientific). For CpG treatment, 8-week-old mice were injected i.p., every other day for 2 weeks, with 40 μg CpG ODN 2395 (tcgtcgttttcggcgcgcgccg) with phosphorothioate bases (Invitrogen). Serum was collected before treatment, and 6 weeks after treatment. All animal experiments were approved by the Institutional Animal Care and Use Committee at the University of California, San Francisco.

Immunoglobulin and AFC Determination

Quantities of serum and supernatant immunoglobulins (total Ig, IgM, IgG1, IgG2c, IgG2b, IgG3, and IgA) were determined by isotype specific ELISA (Southern Biotechnology). NP (4-Hydroxy-3-nitrophenylacetyl) -specific antibody titers were determined by ELISA with plates coated with NP_{23}-BSA (Biosearch Technologies). dsDNA-specific antibody titers were determined by ELISA with plates coated with Hind III (New England Biolabs) digested pUC19 in 0.1M Tris, overnight at room temperature. Cytokines amounts were measured by ELISA as recommended by the manufacturer (BD Biosciences). Elispot was performed by incubating enriched B cells on plates coated with dsDNA as above. After overnight incubation, plates were washed and incubated with alkaline phosphatase (AP) conjugated anti-IgM (Southern Biotech) and subsequently developed with BCIP substrate (Sigma) dissolved into alkaline phosphatase buffer (0.1M Tris, 0.1 M NaCl, and 5 mM $MgCl_2$) and 0.6% LMP Agarose (Sigma).

Autoantigen arrays were printed and processed as previously described. Arrays were probed with goat antibody specific for mouse Ig (Jackson Immunoresearch). Detailed protocols and lists of antigens have been published and are available online at http://utzlab.stanford.edu/protocols (Robinson et al., 2002). Significance analysis of microarrays (SAM) was applied to the data for identification of antigens with statistically significant differences in array reactivity between mutant and wild-type mice (Tusher et al., 2001).

Histology and Immunohistochemistry

Kidneys and spleens were fixed in 10% formalin. Sections and H&E stain were performed by the UCSF VAMC Pathology Core. For immunohistochemistry, kidneys were embedded in Tissue-Tek OCT compound and snap frozen in methyl-butane with dry ice. Tissue sections were then stained with IgM-FITC or IgG-FITC (Jackson Immunoresearch) or with IgG2c-FITC or IgG2b-FITC (Bethyl Laborotories).

Cell Signaling Assays

Enriched B cells were stimulated as indicated in the figures and lysed in 0.1% NP-40 (Calbiochem) lysis buffer, and nuclei were spun down so that cytoplasmic lysates were produced. Lysates were cleared by centrifugation at 14,000 g for 20 min at 4°C, supernatants were removed, heated in Laemmli buffer and run on SDS-PAGE (Novex System, Invitrogen). Immunoblots were probed for A20 (Boone et al., 2004), actin (JLA20, Calbiochem), phospho-IκBα, IκBα, phospho-Erk, Erk, phospho-NF-κB2 p100 and NF-κB2 p100/p52 (Cell Signaling), and Bcl-x (Transduction Biotechnologies).

Fas-Induced Cell Death Assay

Fas-induced cell death assays were performed as described (Watanabe et al., 1995; Wang et al., 1996). In brief, enriched B cells were plated with agonist anti-CD40 (1 μg/ml) for 60 hr. Agonist anti-CD95 (Fas) was added to the cultures at the indicated doses for the last 12 hr. Cells were harvested and stained for flow cytometry with Annexin-V (BD Biosciences) and DAPI.

Real-Time PCR Assays

For quantitation of genomic *Tnfaip3* exon 2, DNA was prepared with the DNeasy Kit (QIAGEN), after which qPCR was performed with SYBR Green (QIAGEN). Primers for exon 2 of *Tnfaip3* were the following: 5′-CTGACCTGGTCCTGAGGAAG-3′ (sense); and 5′-GCAAAGTCCTGTTTCCA CAA-3′ (anti-sense). This qPCR assay was shown to detect less than 1% of exon 2 DNA in titrated mixtures of $Tnfaip3^{-/-}$ and $Tnfaip3^{+/+}$ cells (data not shown). For quantitation of Bcl-x mRNA expression, mRNA was prepared with RNeasy Kit (QIAGEN) and cDNA was obtained with Quantitect Reverse Transcription Kit (QIAGEN). Primers for Bcl-x cDNA were the following: 5′-GCAGACCCAGTAAGTGAGCA-3′ (sense) and 5′-AGAAAGTCGACCACCAG CTC-3′ (antisense). In both types of assays, β-actin primers used as a reference were: 5′- AAGTGTGACGTTGACATCCGTAA-3′ (sense) and 5′-TGCC TGGGTACATGGTGG TA-3′ (antisense). Assays were performed with an ABI 7300 real-time PCR machine (Applied Biosystems).

SUPPLEMENTAL INFORMATION

Supplemental Information includes two figures and can be found with this article online at doi:10.1016/j.immuni.2010.07.017.

ACKNOWLEDGMENTS

This work was supported by the National Institutes of Health, the Alliance for Lupus Research (A.M.), the Fundação para a Ciência e Tecnologia (to R. T.), UCSF-VAMC Pathology Core, the Cancer Center Pathology Core, UCSF Liver Center Immunology and Pathology Cores, the UCSF Transgenic and Targeted Mutagenesis Core Facility, and the Rainin Foundation. We thank the skillful technical assistance of I. Hsieh (UCSF-VAMC Pathology) and J. Publicover (UCSF Liver Center), and helpful advice from J.P. Pereira and L. Reinhardt. We thank T. DeFranco and J. Cyster for critically reading the manuscript. R.M.T. planned and performed the experiments, analyzed the data, and assisted in writing the manuscript. E.E.T. made the conditional gene targeting construct, performed gene targeting in ESCs, and characterized the original $Tnfaip3^{fl}$ germline mice. R.A. performed mice breeding and genotyping, and assisted with mouse injections and bleeding. C.L.L. performed the antibody array experiments and statistical analyses, under the supervision of P.J.U. C.A.L., and P.J.U. edited the manuscript. P.S. assisted in the analysis of the autoantibody data and mouse histology and immunohistochemistry, under the supervision of C.A.L. L.R. performed some of the initial experiments with R.M.T. J.B. provided excellent technical assistance. B.A.M. and A.M. helped plan and supervise the experiments and data analysis and wrote the manuscript.

Received: January 22, 2010
Revised: May 27, 2010
Accepted: July 27, 2010
Published online: August 12, 2010

REFERENCES

Arvelo, M.B., Cooper, J.T., Longo, C., Daniel, S., Grey, S.T., Mahiou, J., Czismadia, E., Abu-Jawdeh, G., Ferran, C., and Ferran, C. (2002). A20 protects mice from D-galactosamine/lipopolysaccharide acute toxic lethal hepatitis. Hepatology *35*, 535–543.

Boone, D.L., Turer, E.E., Lee, E.G., Ahmad, R.C., Wheeler, M.T., Tsui, C., Hurley, P., Chien, M., Chai, S., Hitotsumatsu, O., et al. (2004). The ubiquitin-modifying enzyme A20 is required for termination of Toll-like receptor responses. Nat. Immunol. *5*, 1052–1060.

Cappione, A., 3rd, Anolik, J.H., Pugh-Bernard, A., Barnard, J., Dutcher, P., Silverman, G., and Sanz, I. (2005). Germinal center exclusion of autoreactive B cells is defective in human systemic lupus erythematosus. J. Clin. Invest. *115*, 3205–3216.

Compagno, M., Lim, W.K., Grunn, A., Nandula, S.V., Brahmachary, M., Shen, Q., Bertoni, F., Ponzoni, M., Scandurra, M., Califano, A., et al. (2009). Mutations of multiple genes cause deregulation of NF-kappaB in diffuse large B-cell lymphoma. Nature *459*, 717–721.

Coornaert, B., Baens, M., Heyninck, K., Bekaert, T., Haegman, M., Staal, J., Sun, L., Chen, Z.J., Marynen, P., and Beyaert, R. (2008). T cell antigen receptor stimulation induces MALT1 paracaspase-mediated cleavage of the NF-kappaB inhibitor A20. Nat. Immunol. *9*, 263–271.

Düwel, M., Welteke, V., Oeckinghaus, A., Baens, M., Kloo, B., Ferch, U., Darnay, B.G., Ruland, J., Marynen, P., and Krappmann, D. (2009). A20 negatively regulates T cell receptor signaling to NF-kappaB by cleaving Malt1 ubiquitin chains. J. Immunol. *182*, 7718–7728.

Ehlers, M., Fukuyama, H., McGaha, T.L., Aderem, A., and Ravetch, J.V. (2006). TLR9/MyD88 signaling is required for class switching to pathogenic IgG2a and 2b autoantibodies in SLE. J. Exp. Med. *203*, 553–561.

Elgueta, R., Benson, M.J., de Vries, V.C., Wasiuk, A., Guo, Y., and Noelle, R.J. (2009). Molecular mechanism and function of CD40/CD40L engagement in the immune system. Immunol. Rev. *229*, 152–172.

Fairhurst, A.-M., Wandstrat, A.E., and Wakeland, E.K. (2006). Systemic lupus erythematosus: Multiple immunological phenotypes in a complex genetic disease. Adv. Immunol. *92*, 1–69.

Fukuyama, H., Adachi, M., Suematsu, S., Miwa, K., Suda, T., Yoshida, N., and Nagata, S. (2002). Requirement of Fas expression in B cells for tolerance induction. Eur. J. Immunol. *32*, 223–230.

Graham, R.R., Cotsapas, C., Davies, L., Hackett, R., Lessard, C.J., Leon, J.M., Burtt, N.P., Guiducci, C., Parkin, M., Gates, C., et al. (2008). Genetic variants near *TNFAIP3* on 6q23 are associated with systemic lupus erythematosus. Nat. Genet. *40*, 1059–1061.

Grillot, D.A., Merino, R., Pena, J.C., Fanslow, W.C., Finkelman, F.D., Thompson, C.B., and Nunez, G. (1996). bcl-x exhibits regulated expression during B cell development and activation and modulates lymphocyte survival in transgenic mice. J. Exp. Med. *183*, 381–391.

Hao, Z., Duncan, G.S., Seagal, J., Su, Y.-W., Hong, C., Haight, J., Chen, N.-J., Elia, A., Wakeham, A., Li, W.Y., et al. (2008). Fas receptor expression in germinal-center B cells is essential for T and B lymphocyte homeostasis. Immunity *29*, 615–627.

Hayden, M.S., and Ghosh, S. (2008). Shared principles in NF-kappaB signaling. Cell *132*, 344–362.

Hitotsumatsu, O., Ahmad, R.C., Tavares, R., Wang, M., Philpott, D., Turer, E.E., Lee, B.L., Shiffin, N., Advincula, R., Malynn, B.A., et al. (2008). The ubiquitin-editing enzyme A20 restricts nucleotide-binding oligomerization domain containing 2-triggered signals. Immunity *28*, 381–390.

Hömig-Hölzel, C., Hojer, C., Rastelli, J., Casola, S., Strobl, L.J., Müller, W., Quintanilla-Martinez, L., Gewies, A., Ruland, J., Rajewsky, K., and Zimber-Strobl, U. (2008). Constitutive CD40 signaling in B cells selectively activates the noncanonical NF-kappaB pathway and promotes lymphomagenesis. J. Exp. Med. *205*, 1317–1329.

Jacobi, A.M., and Diamond, B. (2005). Balancing diversity and tolerance: Lessons from patients with systemic lupus erythematosus. J. Exp. Med. *202*, 341–344.

Kato, M., Sanada, M., Kato, I., Sato, Y., Takita, J., Takeuchi, K., Niwa, A., Chen, Y., Nakazaki, K., Nomoto, J., et al. (2009). Frequent inactivation of A20 in B-cell lymphomas. Nature *459*, 712–716.

Klein, U., and Dalla-Favera, R. (2008). Germinal centres: Role in B-cell physiology and malignancy. Nat. Rev. Immunol. *8*, 22–33.

Krikos, A., Laherty, C.D., and Dixit, V.M. (1992). Transcriptional activation of the tumor necrosis factor alpha-inducible zinc finger protein, A20, is mediated by kappa B elements. J. Biol. Chem. *267*, 17971–17976.

Lee, E.G., Boone, D.L., Chai, S., Libby, S.L., Chien, M., Lodolce, J.P., and Ma, A. (2000). Failure to regulate TNF-induced NF-kappaB and cell death responses in A20-deficient mice. Science *289*, 2350–2354.

Mizuno, T., Zhong, X., and Rothstein, T.L. (2003). Fas-induced apoptosis in B cells. Apoptosis *8*, 451–460.

Musone, S.L., Taylor, K.E., Lu, T.T., Nititham, J., Ferreira, R.C., Ortmann, W., Shifrin, N., Petri, M.A., Kamboh, M.I., Manzi, S., et al. (2008). Multiple polymorphisms in the *TNFAIP3* region are independently associated with systemic lupus erythematosus. Nat. Genet. *40*, 1062–1064.

Novak, U., Rinaldi, A., Kwee, I., Nandula, S.V., Rancoita, P.M., Compagno, M., Cerri, M., Rossi, D., Murty, V.V., Zucca, E., et al. (2009). The NF-kappaB negative regulator *TNFAIP3* (A20) is inactivated by somatic mutations and genomic deletions in marginal zone lymphomas. Blood *113*, 4918–4921.

Opipari, A.W., Jr., Boguski, M.S., and Dixit, V.M. (1990). The A20 cDNA induced by tumor necrosis factor alpha encodes a novel type of zinc finger protein. J. Biol. Chem. *265*, 14705–14708.

Rathmell, J.C., Cooke, M.P., Ho, W.Y., Grein, J., Townsend, S.E., Davis, M.M., and Goodnow, C.C. (1995). CD95 (Fas)-dependent elimination of self-reactive B cells upon interaction with CD4+ T cells. Nature *376*, 181–184.

Rickert, R.C., Roes, J., and Rajewsky, K. (1997). B lymphocyte-specific, Cre-mediated mutagenesis in mice. Nucleic Acids Res. *25*, 1317–1318.

Robinson, W.H., DiGennaro, C., Hueber, W., Haab, B.B., Kamachi, M., Dean, E.J., Fournel, S., Fong, D., Genovese, M.C., de Vegvar, H.E., et al. (2002). Autoantigen microarrays for multiplex characterization of autoantibody responses. Nat. Med. *8*, 295–301.

Sarma, V., Lin, Z., Clark, L., Rust, B.M., Tewari, M., Noelle, R.J., and Dixit, V.M. (1995). Activation of the B-cell surface receptor CD40 induces A20, a novel zinc finger protein that inhibits apoptosis. J. Biol. Chem. *270*, 12343–12346.

Schmidt-Supprian, M., and Rajewsky, K. (2007). Vagaries of conditional gene targeting. Nat. Immunol. *8*, 665–668.

Schmitz, R., Hansmann, M.L., Bohle, V., Martin-Subero, J.I., Hartmann, S., Mechtersheimer, G., Klapper, W., Vater, I., Giefing, M., Gesk, S., et al. (2009). *TNFAIP3* (A20) is a tumor suppressor gene in Hodgkin lymphoma and primary mediastinal B cell lymphoma. J. Exp. Med. *206*, 981–989.

Schram, B.R., and Rothstein, T.L. (2003). NF-kappa B is required for surface Ig-induced Fas resistance in B cells. J. Immunol. *170*, 3118–3124.

Sen, R. (2006). Control of B lymphocyte apoptosis by the transcription factor NF-kappaB. Immunity *25*, 871–883.

Shlomchik, M.J. (2008). Sites and stages of autoreactive B cell activation and regulation. Immunity *28*, 18–28.

Siebenlist, U., Brown, K., and Claudio, E. (2005). Control of lymphocyte development by nuclear factor-kappaB. Nat. Rev. Immunol. *5*, 435–445.

Skaug, B., Jiang, X., and Chen, Z.J. (2009). The role of ubiquitin in NF-kappaB regulatory pathways. Annu. Rev. Biochem. *78*, 769–796.

Smith, K.G.C., Nossal, G.J.V., and Tarlinton, D.M. (1995). FAS is highly expressed in the germinal center but is not required for regulation of the B-cell response to antigen. Proc. Natl. Acad. Sci. USA *92*, 11628–11632.

Takahashi, Y., Cerasoli, D.M., Dal Porto, J.M., Shimoda, M., Freund, R., Fang, W., Telander, D.G., Malvey, E.N., Mueller, D.L., Behrens, T.W., and Kelsoe, G. (1999). Relaxed negative selection in germinal centers and impaired affinity maturation in bcl-xL transgenic mice. J. Exp. Med. *190*, 399–410.

Takahashi, Y., Ohta, H., and Takemori, T. (2001). Fas is required for clonal selection in germinal centers and the subsequent establishment of the memory B cell repertoire. Immunity *14*, 181–192.

Turer, E.E., Tavares, R.M., Mortier, E., Hitotsumatsu, O., Advincula, R., Lee, B., Shifrin, N., Malynn, B.A., and Ma, A. (2008). Homeostatic MyD88-dependent signals cause lethal inflamMation in the absence of A20. J. Exp. Med. *205*, 451–464.

Tusher, V.G., Tibshirani, R., and Chu, G. (2001). Significance analysis of microarrays applied to the ionizing radiation response. Proc. Natl. Acad. Sci. USA *98*, 5116–5121.

von Boehmer, H., and Melchers, F. (2010). Checkpoints in lymphocyte development and autoimmune disease. Nat. Immunol. *11*, 14–20.

Wang, J., Taniuchi, I., Maekawa, Y., Howard, M., Cooper, M.D., and Watanabe, T. (1996). Expression and function of Fas antigen on activated murine B cells. Eur. J. Immunol. *26*, 92–96.

Watanabe, D., Suda, T., and Nagata, S. (1995). Expression of Fas in B cells of the mouse germinal center and Fas-dependent killing of activated B cells. Int. Immunol. *7*, 1949–1956.

Wertz, I.E., O'Rourke, K.M., Zhou, H., Eby, M., Aravind, L., Seshagiri, S., Wu, P., Wiesmann, C., Baker, R., Boone, D.L., et al. (2004). De-ubiquitination and ubiquitin ligase domains of A20 downregulate NF-kappaB signalling. Nature *430*, 694–699.

William, J., Euler, C., Christensen, S., and Shlomchik, M.J. (2002). Evolution of autoantibody responses via somatic hypermutation outside of germinal centers. Science *297*, 2066–2070.

Witte, T. (2008). IgM antibodies against dsDNA in SLE. Clin. Rev. Allergy Immunol. *34*, 345–347.

Yurasov, S., and Nussenzweig, M.C. (2007). Regulation of autoreactive antibodies. Curr. Opin. Rheumatol. *19*, 421–426.